

Computational Investigation of Magnetohydrodynamics Boundary of Maxwell Fluid Across Nanoparticle-Filled Sheet

Taseer Muhammad¹, Hijaz Ahmad²*, Umar Farooq³, Ali Akgül⁴

¹King Khalid University This link is disabled., Abha, Saudi Arabia

²Section of Mathematics, International Telematic University Uninettuno, Corso Vittorio Emanuele, Roma, Italy

³ Department of Mathematics, Government College University Faisalabad, Faisalabad, 38000, Pakistan

⁴ Siirt Üniversitesi, Siirt, Turkey

*Corresponding Author: Hijaz Ahmad

DOI: <https://doi.org/10.55145/ajest.2023.02.02.011>

Received February 2023; Accepted April 2023; Available online April 2023;

ABSTRACT: This article examines a flow of a boundary layer as well as a temperature exchange of Maxwell-fluid in 2D along an expansion sheet using numerical methods. The impacts of magnetohydrodynamics (MHD) plus stretch on an inflow are taken into account. Methods in which nanoparticles might damage the environment are also investigated. we present differential transform method that can be applied to transform nonlinear partial differential equation into connected ODEs. A boundary layer Equations formula. are resolved numerically utilizing the Maxwell-nanofluid model. Emerging variables constraint that affects concentration and also on temp profile alone are studied; they include a magnetic constraint M , stretchy constraint K , Prandtl constraint Pr , Mass transfer restriction Nb , a convective heat flow constraint Nt , and Lewis No . Le . Interesting graphs of a findings are displayed. There are also correlations between a flow control factors and coefficient of skin friction, a dimensionless heat exchange amount, and the concentrate amount.

Keywords: Maxwell-fluid, Magnetohydrodynamics, Nanoparticle-Filled, Heat Flow.

1. INTRODUCTION

Since non-Newtonian fluids have so many industrial and manufacturing applications, there has been a spike in interest in researching their boundary layer fluxes. Drilling muds, thermoplastic polymers, optical fibers, metal spinning, cooling metallic plates in cooling baths, as well as the production of hot rolling paper are some examples. Researchers have provided many models in the past Since non-Newtonian materials defy description through any existing model. These prototypes can be generically categorized as differentially amount, or integral fluids. The studied amount -type fluid belongs to the category of Maxwell fluids. This fluid model predicts that the effects of relaxation time could be anticipated. Differential fluids are incapable of forecasting these outcomes. At [1] Double diffusive flow of a Maxwell fluid via a porous medium and its stability analysis were presented. At [2] investigated the thermophoretic and redox processes associated with the Maxwell fluid's MHD flow past a vertical stretched sheet. At [3] investigated the behavior of a suddenly shifted flat surface in a viscous incompressible utilizing a Maxwell prototypical. At [4] examined a flow of an upper converted Maxwell fluid across a porous shrinking sheet, taking into consideration both MHD and heat transmission. Mukhopadhyay [5] investigated the turbulent movement of a Maxwell fluid which produces and absorbs heat.

Flow induced by the stretching of a sheet has been investigated on purpose due to production of polymer sheets, filaments, as well as wires are just a few examples of its many industrial uses, it is assumed that the moving layer expands in its own plane and has both thermal and mechanical interactions with the fluid medium. There are numerous types of materials that undergo stretching and contracting, and each has its own particular strengths, transparency ranges, as well as sheen levels. Initially, at [6] presented the idea of the flow of boundaries on a stretch sheet. At [7] extended a notion originally proposed via made it applicable to sheets that extend linearly and exponentially. Recent research has focused heavily on low flow across a stretchable surface. Recent investigations have been conducted in this direction, with a range of results recorded in Refs [8–14].

Power generators, Magnetohydrodynamic accelerators, exchangers, including electrostatic filters can all benefit from using fluids that transmit electricity. In metallurgy, cooling of uninterrupted strips and filaments drawn thru a static fluid and purifying molten materials from nonmetallic impurities are two examples of the use of fluid flow, such considerations are especially important in stretching flows. The amount of cooling can be altered when the strips are dragged through a magnetic field applied to an electrically conducting fluid [15].

Recent scientific study has focused on nanofluids. Nanofluids are composed of a base liquid and nanoparticles that are thoroughly combined. The word "nanofluid" was created by [16] to describe synthetic colloids composed of nanoparticles floating in a liquid. Maxwell is credited with developing Dispersing solid in fluid to promote heat transfer in the 1800s. Nanoparticles can stay suspended indefinitely if kept below a certain concentration and/or changed with surface/stabilizers, outlasting their micro-sized counterparts. Nanoparticles have a million times more surface area to volume ratio than micro particles, and more surface atoms. By using these features, stable suspensions with improved flow, heat transfer, as well as other properties can be made. Base fluids include water, organic solvent, oil, bio-fluids, and polymer solutions. Oxide ceramic (Al₂O₃, CuO), metal nanotubes (AlN, SiN), cement ceramic (TiC, SiC), silver, copper, platinum, various types of carbon (e.g., diamond, carbon, carbon nanotube, fullerene) can be utilized to manufacture nanoparticles.

At [17-20] studied how nanoparticles affected boundary layer flow over a vertical plate. Authors analyze nanofluid flow via a vertical plate in a flow boundary layer. New studies [21] has expanded the authors' notion to include the investigation of nanofluid boundary layer flow across an extended sheet at a specific temperature. [22] then studied nanofluid boundary layer flow over a vibrating structure in a moving fluid. [23] used the concept of a nanofluid to explain that flow of a dual-diffusive spontaneous flow boundary layer in a nanofluid-saturated porous medium across a vertical surface with such a given surface temperature and solute as well as nanoparticle fluxes. Recent study [24] evaluated the influence of a nanofluid on exponentially stretched boundary layer flow. Using a variety of fluid models, researchers [25–30] study nanofluids.

This research focuses on nanofluids including their impact on non-Newtonian Maxwell-fluids in magnetohydrodynamics (MHD). We solve nondimensionalized equations using similarity transforms and numerical methods. Examples are K, M, Pr, Nb, Nt, Le, and Le. A main objective is to discover how modifying a control constraint effects a distribution of velocities, temperatures, and nanoparticles. The impact of altering the MHD constraint and the non-Newtonian constraint on quickness is depicted graphically. For a range of nanofluid constraint values, graphs depicting the increase in temperature and nanoparticle concentration are also provided. All three factors, $(1 + K)f'(0)$, $\Theta'(0)$, and $\Phi'(0)$, are determined to match past research.

2. Definition of the Problem

Consider a sheet getting stretched in 2D and the fluid flowing past it as a constant, incompressible fluid. When the sheet is stretched in the $y = 0$ plane, both the MHD and nanoparticle effects are at their peak. We assume the flow is bounded above and below the y axis at 0 degrees. Let's suppose, for the purpose of this discussion, that the sheet is being stretched at a continuous linear quickness, $u(x) = ax$, with the x -axis parallel to the stretching surface as well as a > 0 . A consistent of magnetic field is used to a prolonged surface. The magnetic field generated has hardly no effect. The fluid boundary layer eq of Maxwell for a nanofluid containing particles are [2].

$$\frac{du}{dx} + \frac{dy}{dy} = 0, \tag{1}$$

$$u \frac{du}{dx} + v \frac{du}{dy} = \nu \left(\frac{d^2u}{dy^2} \right) + k_0 \left(u^2 \frac{d^2u}{dx^2} + v^2 \frac{d^2u}{dy^2} + 2uv \frac{d^2u}{dy^2} \right) - \frac{\sigma B^2}{\rho f} \left(u + k_0 v \frac{du}{dy} \right) \tag{2}$$

$$u \frac{dT}{dx} + v \frac{dT}{dy} = \alpha \left(\frac{d^2T}{dx^2} + \frac{d^2T}{dy^2} \right) + \tau D_B \left\{ \left(\frac{dC}{dx} \frac{dT}{dx} + \frac{dC}{dy} \frac{dT}{dy} \right) + \left(\frac{dT}{d\infty} \right) \left[\frac{dT}{dx} + \frac{dT}{dy} \right] \right\} \tag{3}$$

$$u \frac{dC}{dx} + v \frac{dC}{dy} = D_B \left(\frac{d^2C}{dx^2} + \frac{d^2C}{dy^2} \right) + \left(\frac{dT}{d\infty} \right) \left(\frac{d^2T}{dx^2} + \frac{d^2T}{dy^2} \right) \tag{4}$$

Where u and v are x and y motions, ν is a base fluid viscosity, α is a fluid's kinematic viscosity, s is a conductivity, ρ is a density of a fluid, B_0 is a magnetic inducement, k_0 is a UCM fluid's relaxation time, and τ is thermal diffusivity. T is a fluid temp, C is nanoparticle percentage, T as well as C exist nanoparticle temp in addition to concentration, respectively. The (τ) is thermophoretic flow constant (C) f is ratio among an efficient heat capacity of a nanoparticle material and a fluid's heat capacity; C is a volumetric volume expansion coefficient; as well as ρ is a particle density. As y approaches infinity, the ambient temperatures and pressures are denoted via T_∞ then C_∞ , respectively. A specific boundary conditions for Eq. (2) to (4) are:

$$u = u_w(x) = ax, \quad v = 0, \quad T = Tw, \quad C = Cw \quad \text{at } y = 0, \quad u = 0, \quad v = 0, \quad T = T\infty, \quad C = C\infty, \quad \text{as } y \rightarrow \infty \quad (5)$$

$$\Psi = (\alpha v)^{1/2} x f(\eta), \quad \theta(\eta) = \frac{T-T\infty}{Tw-T\infty} \quad (6)$$

$$\phi(\eta) = \frac{C-C\infty}{Cw-C\infty}, \quad \eta = \sqrt{\frac{\alpha}{\nu}} y,$$

where the function stream c is defined Utilizing Eq. [6], A continuity equation is identically satisfied, & Equations. (2) to (4) in [5] have the check on form:

$$f''' - (M^2)f' - (f')^2 (1 + MK)ff'' + K(f^2 f''' - 2 f f' f''') = 0 \quad (7)$$

$$\theta'' + Pr[f\theta' + Nb(\theta'\theta') + Nt(\theta')^2] \quad (8)$$

$$\phi'' + LePr (f\phi') + \frac{Nt}{Nb} \theta'' = 0 \quad (9)$$

$$f(0) = 0, \quad f'(0) = 1, \quad f'(\infty) = 0, \quad (10)$$

$$\theta(0) = 1, \quad \theta(\infty) = 0, \quad (11)$$

$$\phi(0) = 1, \quad \phi(\infty) = 0, \quad (12)$$

Cf, Nu, and Sh are all related in the equations to one another (13-14).

$$Cf = \frac{\tau w}{\rho u_w^2(x)}, \quad Nu = \frac{xq_w}{\alpha(Tw-T\infty)}, \quad sh = \frac{xq_m}{D_B(Cw-C\infty)} \quad (13)$$

$$\tau w = u(1 + k) \frac{du}{dy}, \quad q_w = -\alpha \left(\frac{dT}{dy}\right), \quad q_m = -D_B \left(\frac{dC}{dy}\right) \quad (14)$$

$$R_{ex}^{\frac{1}{2}} Cf = (1 + K)f''(0), \quad R_{ex}^{\frac{1}{2}} Nu = -\theta'(0), \quad R_{ex}^{\frac{1}{2}} sh = -\phi'(0) \quad (15)$$

3. Outcomes and Discussions

By means of a 4th order (Runge-Kutta-Fehlberg) approach, we have numerically solved the boundary value issues associated with nonlinear coupled ODE. (7) to (9) which are constrained by some external force (10) to (12). Referring to the speed distribution $f(\eta)$, temp profile $\theta(\eta)$, as well as a nanoparticle fraction (ϕ), Figures. 1 to 6 depict the performance of an evolving constraints, with the magnetic limitations M , flexible limits K , Prandtl constraint Pr , Brownian constraint Nb , thermophoresis constraint Nt , and Lewis No. Le (η).

Figure 1 shows the results obtained for changed amounts of M , magnetic constraint, quickness, temp, as well as proportion of nanoparticles, while keeping all other constraint at their default levels. Figure 1 shows that as M was increased, temp profile and fraction of nanoparticles both rose. A quickness profile $f(\eta)$, however, exhibits a diminishing pattern for rising amounts of M . (show Figure. 1).

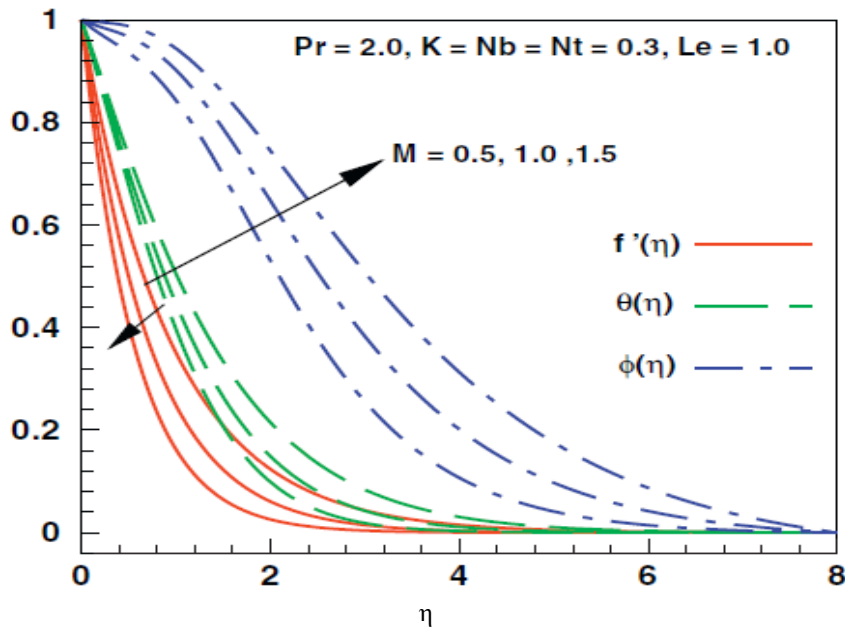


FIGURE 1. - Impacts of M on quickness profile $f(\eta)$, temp profile $\Theta(\eta)$, as well as strength profile are introduced $\emptyset(\eta)$.

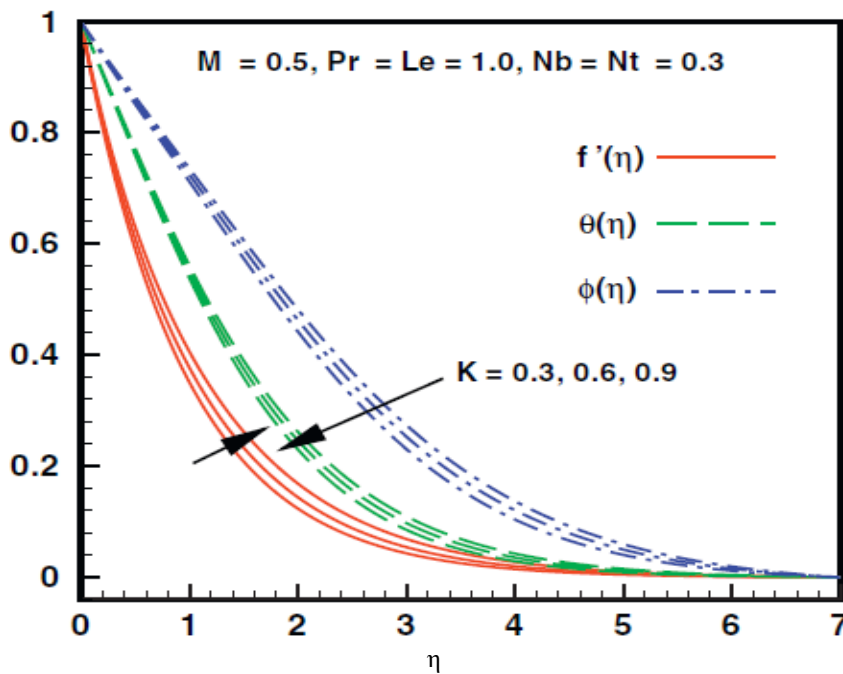


FIGURE 2. - Impacts of K on quickness profile $f(\eta)$, temp profile $\Theta(\eta)$, as well as strength profile are introduced $\emptyset(\eta)$.

In contrast, the boundary layer becomes thinner, As M increases, fluid temperature, nanoparticle fraction, and flow resistance rise. M 's compatibility with the fluid. Figure 2 shows that when K grows. When K rises, nanoparticle proportion fall (show Fig. 2). the quickness and temp profiles show an inverse trend with rising K . Constant K reduces boundary layer thickness. Physically, increasing the fluid's elasticity makes it harder to move. When magnetohydrodynamic and non-Newtonian effects are ignored,

Table 1 demonstrates that when magnetohydrodynamic and non-Newtonian effects are disregarded, the results closely match those of Khan and Pop [21]. As demonstrated in Figure 3, both the temperature profile and the proportion of nanoparticles exhibit a decreasing trend in response to Pr . Therefore, boundary layer thickness.

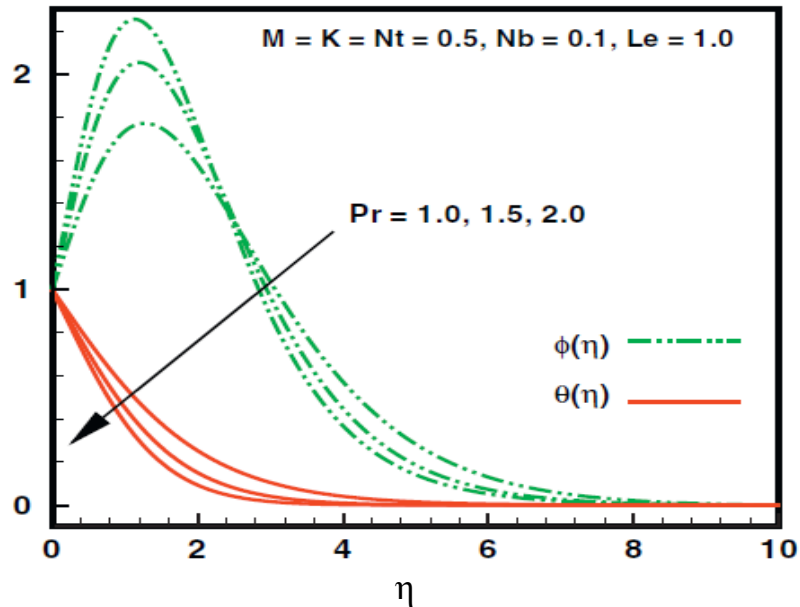


FIGURE 3 - Differences in the $\Theta(\eta)$, and $\phi(\eta)$ temperature distributions as a result of Pr.

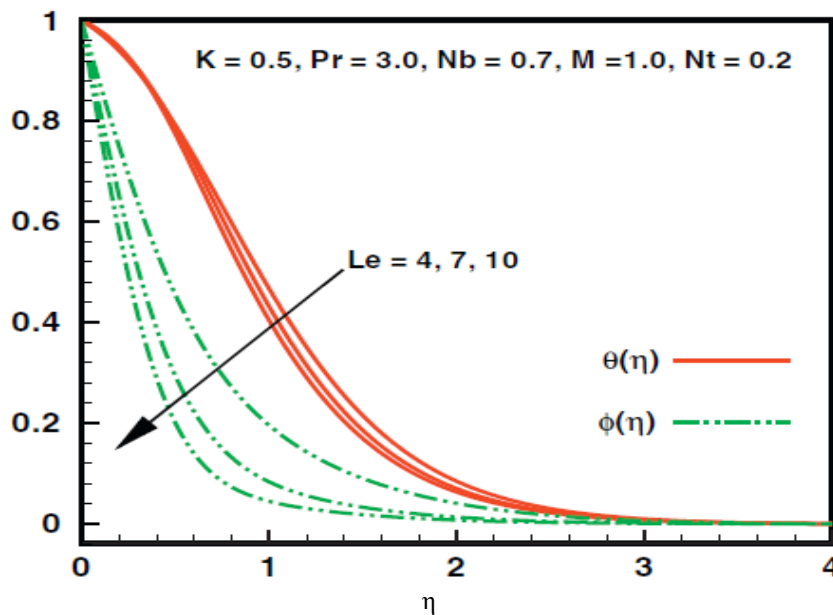


FIGURE 4. - Impact on both the temperature and heat distribution profiles.

Declines indefinitely as Pr is raised. When comparing Figure. 4 with Figure. 3 for larger amount of Le, we see that of temperature as well as the nanoparticle percentage exhibit the same pattern. Figures 5 and 6 depict how the temperature profile $\Theta(\eta)$ and the nanoparticle fraction $\phi(\eta)$ are affected by the Brownian motion and the thermophoresis constraint, respectively. Figures 4 and 5 show that as Nb and Nt are increased, so is a temp profile. While nanoparticle percentage improves with increasing amounts of Nb and Nt in Figure. 5, it does the opposite in Figure. 4. When a result, as Nb and Nt increase, so does the thickness of the boundary layer. Indeed, as can be seen in Table 2, there is a great agreement with Wang [15] when neither nanoparticles nor non-Newtonian effects are present. Presented in Figures. 7 to12 are the relationships between Figure 7 shows skin friction, nusselt No., sherwood No., magnetic constraint, elastic constraint, prandtl constraint, Brownian constraint, thermophoresis constant, and Lewis No., The higher K reduces skin friction.

Figure. 8 displays the relationship between Nusselt No. as well as magnetic constraint M for range of Pr values. The Nusselt and Sherwood No. follow the opposite trend as M and Prandtl No. Pr increase (show Fig. 8). When K is increased, both Nusselt and Sherwood No. show a linear relationship with M. (show Figures. 9 as well as 10). Nusselt No. $\Theta(0)$ is shown to be affected by Brownian constraint Nb for a range of values in Figure. 11.

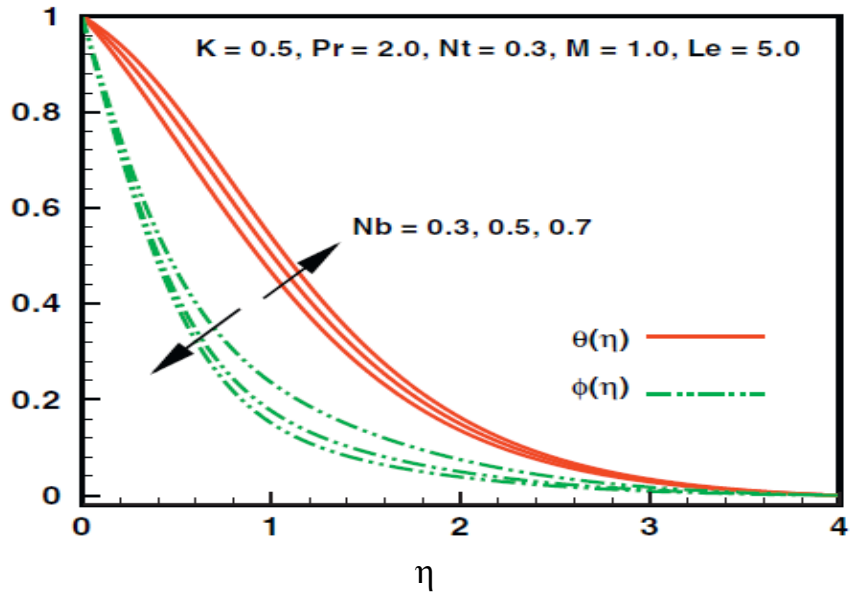


FIGURE 5. - Temperature distribution $\Theta(\eta)$ and temperature distribution $\Phi(\eta)$ as affected by Nb .

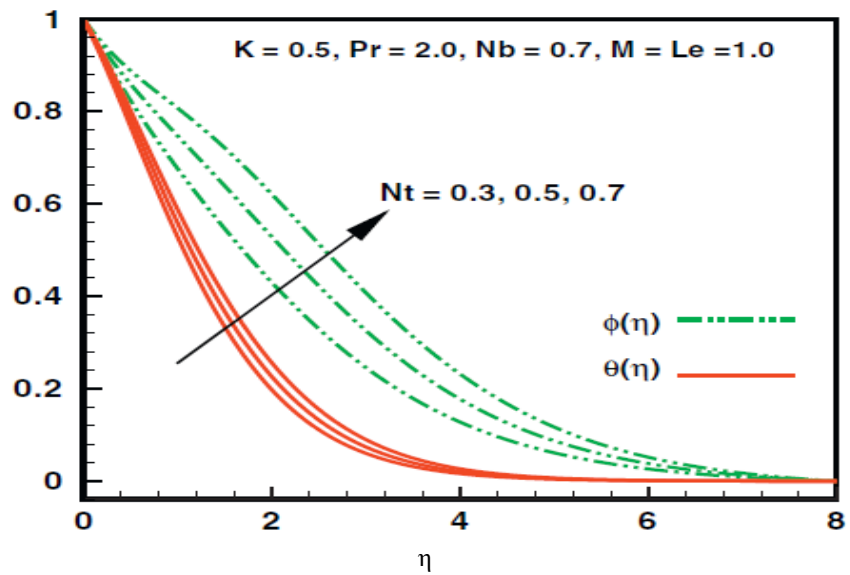


FIGURE 6. - The influence of Nt on the temperature profiles $\Theta(\eta)$ and $\Phi(\eta)$.

Table 1. - Comparison of a local (Nusselt No.) $Re_x^{-1/2} Nux$ as well as a local (Sherwood No.) $Re_x^{-1/2} Sh$ during an absence of both MHD and an elastic constraint when Pr equal ten, Le equal one, and Nb equal 0.1.

Findings at K equal M equal O			At [21]	
$N.t$	$-\Theta(\eta)$	$-\Phi'(\eta)$	$-\Theta(\eta)$	$-\Phi'(\eta)$
0.1	0.95	2.12	0.95	2.12
0.2	0.69	2.27	0.69	2.27
0.3	0.52	2.52	0.52	2.52
0.4	0.40	2.79	0.40	2.79
0.5	0.32	3.03	0.32	3.03

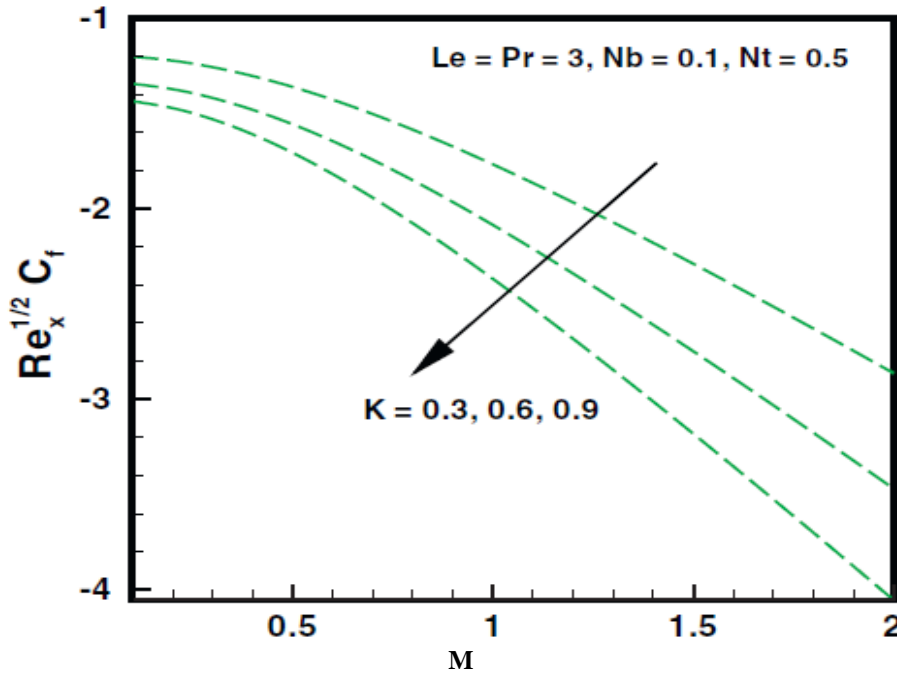


FIGURE 7. - Difference of surface friction factor presented M for differing K amounts.

Table 2. - Comparison of a local (Nusselt No.) $Re_x^{-1/2}$ (Nux numerical) amounts during an absence of MHD, elasticity, as well as nanoparticle fractions.

P.r	Findings at $-\theta'(0)$	At [15]
0.7	0.45	0.45
2	0.95	0.95
7	1.89	1.89
20	3.35	3.35
70	6.46	6.46

Table 3. - With (non-Newtonian fluid), an numerical amounts for a local (Nusselt No.) $Re_x^{-1/2}$ Nux as well as local (S.h No.) $Re_x^{-1/2}$ S.h are $M = K = 0.5$, P.r equal ten, and Le equal one.

N.b	N.t at 0.3		N.t at 0.5		N.t at 0.7	
	$-\theta'(0)$	$-\theta'(0)$	$-\theta'(0)$	$-\theta'(0)$	$-\theta'(0)$	$-\theta'(0)$
0.3	0.13	2.60	0.02	2.49	0.005	2.42
0.5	0.03	2.74	0.017	2.56	0.003	2.47
0.7	0.05	2.84	0.012	2.61	0.002	2.50

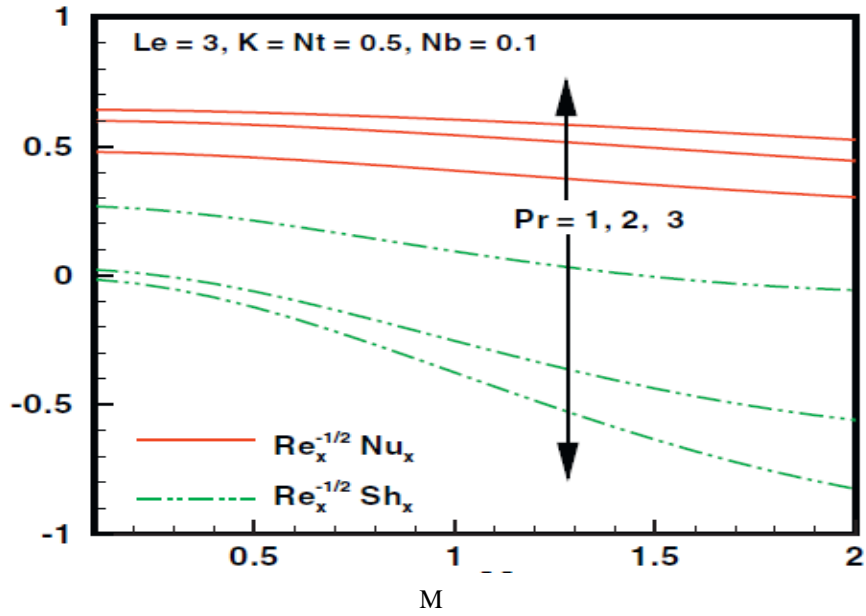


FIGURE 8. - Difference of Nusselt as well as Sh No. s through M for differing amounts of Pr.

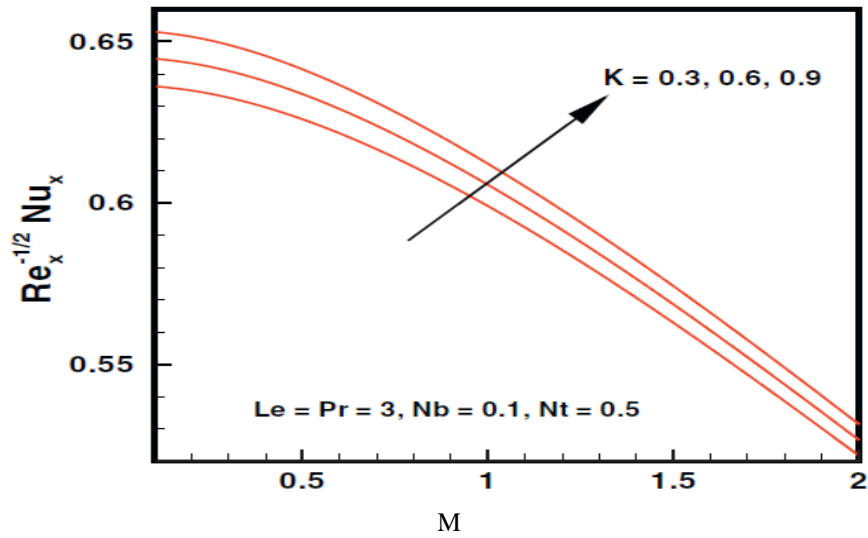


FIGURE 9. - Difference of Nusselt No. for differing k amounts.

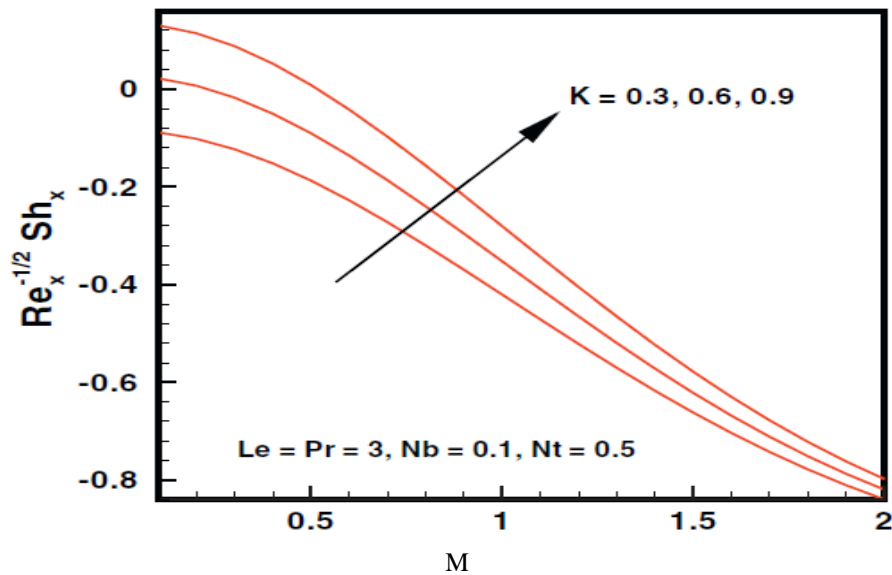


FIGURE 10. - Sh No. difference through M for differing amounts of k.

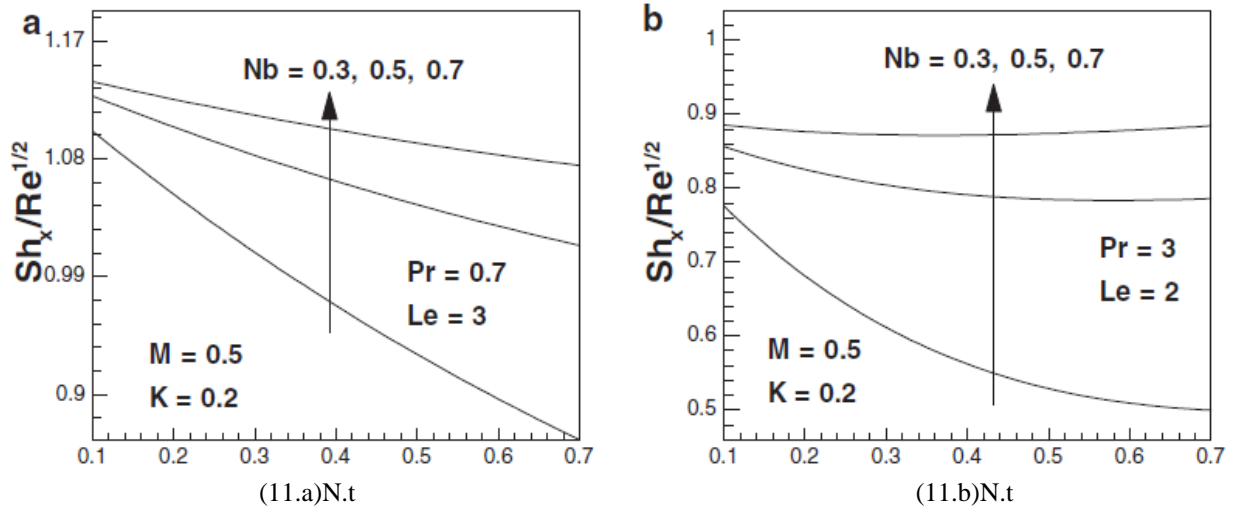


FIGURE 11. - The results of Brownian flow Nb, Prandtl No. Pr, as well as Lewis No. Le on lowered Sh No.

About Pr and Le. When comparing Fig. (11.a) and Fig. (11.b), the Nusselt No. drops off a chart when Nb increases and Pr decreases. At the same time, given a wide range of Prandtl and Lewis No., a larger Brownian motion Nb is associated with an increase in the Sherwood No. $\Theta(\eta)$ (see Fig. 12). Last but not least, high Prandtl values are accompanied by low heat conductivity. As a result, the conduction amount decreases and the heat change amount in sheet's face rises.

4. Conclusions

The effect of the MHD boundary layer flow on a stretching sheet is presented here. constraint for elastic response, Brownian motion, and thermophoresis are all explored in relation to their impacts. The speed, the temperature, and the percentage of nanoparticles are all solved numerically and described. Key findings from the current study are summarized below.

1. The effects of M as well as K on temperature distribution and the distribution of nanoparticles are diametrically opposed.
2. Pr and Le display same behavior with respect to temperature as well as nanoparticle percentage.
3. Nb and Nt have comparable impacts on the temperature distribution.
4. Nb and Nt have opposing effects on the nanoparticle abundance.
5. Nb increases, a magnitude of a local Nusselt No. drops.
6. Magnitude of a local Sherwood No. grows through increasing Nb amounts.

FUNDING

No funding received for this work.

ACKNOWLEDGEMENT

None.

CONFLICTS OF INTEREST

The authors declare no conflict of interest

REFERENCE

- [1] Wang S, Tan WC. Stability analysis of solet-driven double diffusive convection of Maxwell fluid in a porous medium. *Int J Heat Fluid Flow* 2011;32:88–94.
- [2] Noor NFM. Analysis for MHD flow of a Maxwell fluid past a vertical stretching sheet in the presence of thermophoresis and chemical reaction. *World Acad Sci Eng Technol* 2012;64.
- [3] Wenchang T, Mingyu X. plane surface suddenly set in motion in a viscoelastic fluid with maxwell model. *Acta Mech Sin* 2002;18.
- [4] Abel MS, Tawade V, Shinde N. The effects of MHD flow and heat transfer for the UCM fluid over a stretching surface in presence of thermal radiation. *Adv Math Phys* 2012;21:702681.

- [5] Mukhopadhyaya S. Heat transfer analysis of the unsteady flow of a Maxwell fluid over a stretching surface in the presence of a heat source/sink. *Chin Phys Lett* 2012;29:054703.
- [6] Sakiadis BC. Boundary-layer behavior on continuous solid surface: I. Bound-ary-layer equations for two-dimensional and axisymmetric flow. *J Am Inst Chem Eng* 1961;7:26–8.
- [7] Crane L. Flow past a stretching plate. *Zeit Angew Math Phys* 1970;21:645–7.
- [8] Nadeem S, Zaheer S, Fang T. Effects of thermal radiation on the boundary layer flow of a Jeffrey fluid over an exponentially stretching surface. *Num Algo* 2011;57:187–205.
- [9] Nadeem S, Faraz N. Thin film flow of a second grade fluid over a stretching/ shrinking sheet with variable temperature-dependent viscosity. *Chin Phys Lett* 2010;27:034704.
- [10] Nadeem S, Hussain A. HAM solutions for boundary layer flow in the region of the stagnation point towards a stretching sheet. *Commun Nonlinear Sci Numer Simul* 2010;15:475–81.
- [11] Hayat T, Shehzad SA, Qasim M, Obaidat S. Thermal radiation effects on the mixed convection stagnation-point flow in a Jeffery fluid. *Zeit Angew Math Phys* 2011;66:606–14.
- [12] Nadeem, Haq RU, Lee C. MHD flow of a Casson fluid over an exponentially shrinking sheet. *Sci Iran* 2012;19(6):1550–3.
- [13] Chen CH. Magnetohydrodynamic mixed convection of a power law fluid past a stretching sheet in the presence of thermal radiation and internal heat generation/absorption. *Int J Nonlinear Mech* 2009;44:596–603.
- [14] Noor NFM, Kechil SA, Hashim I. Simple non-perturbative solution for MHD viscous flow due to a shrinking sheet. *Commun Nonlinear Sci Numer Simul* 2012;15:144–8.
- [15] Wang CY. Free convection on a vertical stretching surface. *J Appl Math Mech (ZAMM)* 1989;69:418–20.
- [16] Choi SUS. Enhancing thermal conductivity of fluids with nanoparticles. In: *Int. Mech. Eng. Cong. and Exp., ASME, FED 231/MD*, vol. 66; 1995.p. 99–105.
- [17] Nield DA, Kuznetsov AV. The Cheng–Minkowycz problem for natural convective boundary-layer flow in a porous medium saturated by a nanofluid. *Int J Heat Mass Trans* 2009;52:5792–5.
- [18] Kuznetsov AV, Nield DA. Natural convective boundary-layer flow of a nano-fluid past a vertical plate. *Int J Thermal Sci* 2010;49:243–7.
- [19] Nield DA, Kuznetsov AV. The Cheng–Minkowycz problem for the double-diffusive natural convective boundary layer flow in a porous medium satu-rated by a nanofluid. *Int J Heat Mass Trans* 2011;54:374–8.
- [20] Kuznetsov AV, Nield DA. Double-diffusive natural convective boundary-layer flow of a nanofluid past a vertical plate. *Int J Thermal Sci* 2011;50:712–7.
- [21] Khan WA, Pop I. Boundary-layer flow of a nanofluid past a stretching sheet. *Int J Heat Mass Transfer* 2010;53:2477–83.
- [22] Bachok N, Ishak A, Pop I. Boundary-layer flow of nanofluids over a moving surface in a flowing fluid. *Int J Thermal Sci* 2010;49:1663–8.
- [23] Khan WA, Aziz A. Double-diffusive natural convective boundary layer flow in a porous medium saturated with a nanofluid over a vertical plate: Prescribed surface heat, solute and nanoparticle fluxes. *Int J Thermal Sci* 2011;50:2154–60.
- [24] Nadeem S, Lee C. Boundary layer flow of nanofluid over an exponentially stretching surface. *Nanoscale Res Lett* 2012;7(1):94. [25] Makinde OD, Aziz A. Boundary layer flow of a nanofluid past a stretching sheet with a convective boundary condition. *Int J Thermal Sci* 2011;50: 1326–32.
- [26] Sebdani SM, Mahmoodi M, Hashemi S. Effect of nanofluid variable properties on mixed convection in a square cavity. *Int J Thermal Sci* 2012;52:112–26.
- [27] Khan WA, Aziz A. Natural convection flow of a nanofluid over a vertical plate with uniform surface heat flux. *Int J Thermal Sci* 2011;50:1207–14.
- [28] Motsumi TG, Makinde OD. Effects of thermal radiation and viscous dissipation on boundary layer flow of nanofluids over a permeable moving flat plate. *Phys Scr* 2012;86. 045003 (8 pp.).
- [29] Makinde OD. Analysis of Sakiadis flow of nanofluids with viscous dissipation and Newtonian heating. *Appl Math Mech (Engl Ed)* 2012;33(12):1545–54.
- [30] Nadeem S, Haq RU. MHD boundary layer flow of a nanofluid past a porous shrinking sheet with thermal radiation. *J Aerosp Eng* 2012. [http://dx.doi.org/ 10.1061/\(ASCE\)AS.1943-5525.0000299](http://dx.doi.org/10.1061/(ASCE)AS.1943-5525.0000299).